

- 1973.
- (7) T. A. Hahn, *J. Appl. Phys.*, **41**, 5096 (1970).
 - (8) S. Lee, M.S. Thesis, Case Western Reserve University, August 1973.
 - (9) K. H. Illers, *Kolloid-Z. Z. Polym.*, **251**, 394 (1973); **252**, 1 (1974).
 - (10) L. K. McKenna, T. Kajiyama, and W. J. MacKnight, *Macromolecules*, **2**, 58 (1969).
 - (11) V. K. Bergmann and K. Nawotki, *Kolloid-Z. Z. Polym.*, **219**, 131 (1967).
 - (12) J. W. Cooper and N. G. McCrum, *J. Mater. Sci.*, **7**, 1221 (1972).
 - (13) N. G. McCrum, B. Z. Read, and G. Williams, "Anelastic and Dielectric Effects in Polymeric Solids," Wiley, New York, N. Y., 1967.
 - (14) K. Sanui, W. J. MacKnight, and R. W. Lenz, *Macromolecules*, **7**, 101 (1974).
 - (15) R. H. Boyd and S. M. Breitling, *Polym. Prepr., Amer. Chem. Soc., Div. Polym. Chem.*, **14**, 192 (1973).
 - (16) T. E. Schatzki, *Polym. Prepr., Amer. Chem. Soc., Div. Polym. Chem.*, **6**, 646 (1965).
 - (17) R. F. Boyer, *Rubber Chem. Technol.*, **36**, 1303 (1963).
 - (18) H. G. Olf and A. Peterlin, *J. Polym. Sci., Part A-2*, **8**, 791 (1970).
 - (19) E. Baer, R. Kohn, and Y. S. Papir, *J. Macromol. Sci., Phys.*, **6**, 761 (1972).
 - (20) A. Hiltner, E. Baer, J. R. Martin, and J. K. Gillham, *Polym. Prepr., Amer. Chem. Soc., Div. Polym. Chem.*, **13**, 1141 (1972).
 - (21) K. M. Sinnot, *J. Appl. Phys.*, **37**, 3385 (1966); *J. Polym. Sci., Part C*, **14**, 141 (1966).
 - (22) W. Pechhold, V. Eisele, and G. Knauss, *Kolloid-Z. Z. Polym.*, **196**, 27 (1964).
 - (23) T. Kawaguchi, *J. Appl. Polym. Sci.*, **2**, 56 (1959).
 - (24) A. J. Curtis, *J. Res. Nat. Bur. Stand., Sect. A*, **65**, 185 (1961).
 - (25) K. H. Illers, *Kolloid-Z. Z. Polym.*, **191**, 1 (1963); **231**, 622 (1969).
 - (26) A. V. Tobolsky, D. W. Carlson, and N. Indicator, *J. Polym. Sci.*, **54**, 175 (1961).
 - (27) R. F. Boyer, *Macromolecules*, **6**, 288 (1973); *Plast. Polym.*, **41**, 71 (1973).
 - (28) T. Takamatsu and E. Fukada, *Polym. J.*, **1**, 101 (1970).
 - (29) S. S. Chang, *J. Polym. Sci., Part C*, **43**, 43 (1973).

Small Angle Light Scattering by Elastomer-Reinforced Epoxy Resins

S. Visconti and R. H. Marchessault*

Département de Chimie, Université de Montréal, Montréal, Québec H3C 3V1, Canada.

Received May 10, 1974

ABSTRACT: Thermoset epoxy resins can be toughened by means of small elastomeric inclusions. A carboxyl terminated butadiene–acrylonitrile random copolymer (CTBN) was dissolved in a mixture of cycloaliphatic resin with its hardener. The elastomer precipitates during polymerization and small domains of a few microns in size can be viewed in thin sections of the solid polymer after staining with OsO₄. The variation in size and shape of the spherical domains was studied as a function of CTBN content by small angle light scattering and the derived parameters were compared with those obtained *via* transmission electron microscopy. For CTBN concentrations less than 20%, spherical rubber inclusions about 4 μ in size were found by light scattering. Beyond 20%, epoxidic domains are present of about the same size. The morphological changes occurring during polymerization were followed continuously by means of light scattering. It was found that phase separation takes place well before the gelation point and occurs in a time interval which is nearly independent of CTBN concentration. Static deformation of the samples was monitored by light scattering and change in the scattering envelope as a function of elongation was recorded. It was concluded that the spherical domains become ellipsoidal with a tendency toward correlated orientation in the direction of stretch.

Light scattering (LS) analysis of polymer systems is now a well-known tool for quantifying their solid-state morphology. Textural information at the level 0.1–50 μ can be obtained, depending upon the scattering range which is recorded. Two different approaches are available.

If the system has a well-defined superstructure which can be represented by rather simple models, one can use a simulation method. Starting from the amplitude scattered by each element, one draws a theoretical scattering pattern that can be compared to the experimental one for further refinement. This approach has successfully provided a semiquantitative characterization of partially crystalline textures such as spherulites,¹ collagen,² cellulose rods,^{3,4} or even more complex helicoidal fibers.⁵

If the structure is poorly defined, *i.e.*, made of entities of complex shape or with a broad size distribution, a useful treatment is the correlation method originally proposed by Debye and Bueche.⁶ This process relates the scattered intensity to fluctuations⁷ of the dielectric constant (ϵ) inside the material. A correlation function $\gamma(r)$ can be derived from the intensity which correlates the fluctuations η_1 of ϵ at some arbitrary point 1 in the medium with η_2 at some other point 2, a distance r away.

$$\gamma(r) = \langle \eta_1 \eta_2 \rangle / \langle \eta^2 \rangle$$

$\langle \eta^2 \rangle$ = mean square fluctuations, $\langle \eta_1 \eta_2 \rangle$ = average overall possible locations of 1 and 2, r staying constant. The func-

tion $\gamma(r)$ is clearly 1 for $r = 0$ and tends toward 0 for large values of r . If $\gamma(r)$ decreases faster with r for one medium than for another, it means the former is more heterogeneous.

In principle $\gamma(r)$ can be extracted from the intensity data by Fourier inversion. In practice, it is difficult to derive an analytical expression for $\gamma(r)$ when a complex system is involved but it is often possible to fit an exponential $[\exp(-r/a)]$ or a Gaussian $[\exp(-(r/a)^2)]$ function to experimental curves of $\gamma(r)$ vs. r . Determination of the parameter a , which is qualitatively related to the size of the density fluctuations, is then straightforward.

Two more parameters can be defined: an average length of heterogeneity $l_c = 2 \int_0^\infty \gamma(r) dr$, and a volume of heterogeneity $v_c = \int_0^\infty \gamma(r) 4\pi r^2 dr$.

In this paper the scattering of polarized light by rubber-epoxy composites, acrylonitrile–butadiene–epoxy (ABE) network copolymers, will be discussed: in the solid state as a function of rubber concentration, under conditions where the sample is subjected to a static deformation, and during polymerization while phase separation occurs. Both simulation and correlation methods are used for data interpretation.

ABE Composites. The toughening of glassy thermoplastics by addition of small amounts of elastomers has been used for some time to prepare important commercial products such as high impact polystyrene or acrylonitrile–buta-

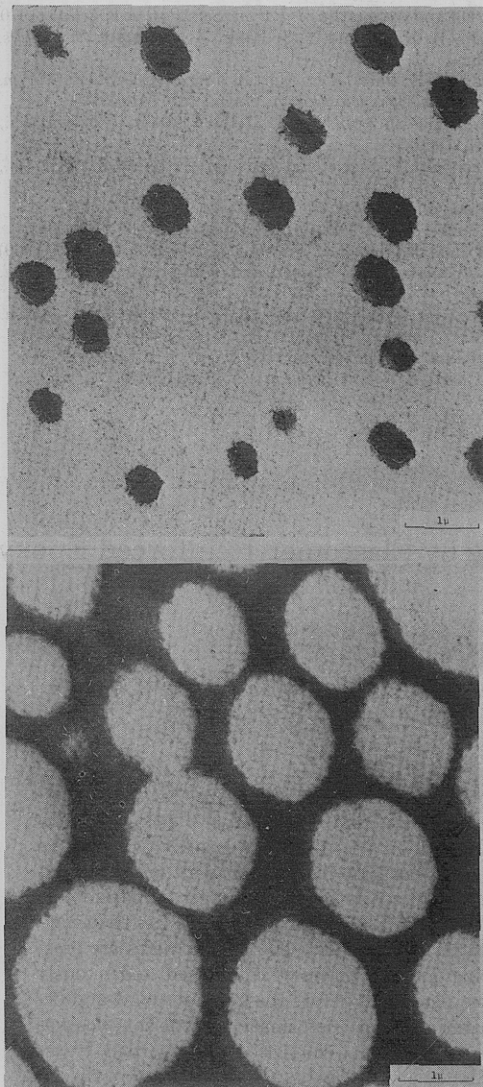


Figure 1. Transmission electron micrographs of a section of ABE resin whose CTBN elastomer is stained with OsO_4 : (top) 9% CTBN; (bottom) 28% CTBN.

diene-styrene (ABS) copolymers. The elastomer is usually dispersed as small domains measuring between 0.1 and 10 μ .⁷ This size being very suitable for light scattering analysis, numerous attempts have been made to use this technique to characterize the morphology of these styrene-butadiene copolymers.⁸⁻¹⁰

More recently, McGarry starting with cycloaromatic epoxy resins¹¹ and Soldatos and Burhans with cycloaliphatic resins¹² developed a similar way to improve the brittle thermoset resins by means of elastomeric inclusions. In both cases, the rubber used was a CTBN (carboxyl terminated butadiene-acrylonitrile random copolymer) of low molecular weight that could be dissolved in the epoxy resin; the curing agent was then added and the mixture cured by heating, giving a so-called ABE copolymer (acrylonitrile-butadiene-epoxy).

Further optimization of the parameters which control the size of the dispersed phase (temperature, type, and amount of curing agent, ...) led to a significant increase in toughness without loss in rigidity.¹²

Transmission electron micrographs^{12,13} of thin OsO_4 stained sections (1000 Å) of the rubber-cycloaliphatic composites show that: in the commercially important range of 2–15% CTBN, by weight (Figure 1, top), the system shows a phase separation with a bimodal distribution of rubber particles, some of them being in the desired micron range



Figure 2. V_v scattering patterns: (left) 14% CTBN; (middle) 20% CN; (right) 28% CTBN.

while much smaller sized particles (~ 200 Å) are uniformly dispersed in the matrix; at about 20% CTBN, a phase inversion begins as evidenced by large domains which stain with OsO_4 ; for 28% CTBN (Figure 1, bottom), the continuous phase is entirely rubbery and contains large occlusions of resins (the size of these occlusions decreases with increasing rubber concentrations). In fact, it has been proposed¹³ that at these high rubber concentrations both epoxy and rubbery phases are continuous and closely intermingled.

From the electron micrographs it is clear that the presence of microphases rich in rubber is a function of the compatibility of the growing macromolecules. Since the starting mixture is homogeneous, phase separation must occur during the polymerization as a result of local compositional differences in the macromolecules at a time when mobility is still possible. It was the obvious need for a textural probe as the polymerization progresses which led us first to use light scattering to characterize this system.

Experimental Section

Procedures. The ABE samples were prepared by mixing equal amounts of epoxy (3,4-epoxycyclohexylmethyl-3,4-epoxycyclohexane carboxylate) and hexahydrophthalic anhydride hardener. To this mixture was added a given fraction of CTBN together with small quantities of benzyldimethylamine and ethylene glycol as catalysts. After manual stirring the homogeneous mixture is then poured into preheated Teflon moulds. The cure cycle starts at 120° for 2 hr followed by 4 hr at 160°.

The moulded bars, generally 2 mm thick, were coated with an immersion fluid (saturated barium iodide solution, n_D 1.53) and mounted between microscope slides, in order to avoid artefacts due to surface scattering.

A classical photographic light scattering apparatus similar to the one described in a previous paper¹⁴ was used: a holder and a photographic plate were placed normal to the incident beam provided by a He-Ne gas laser (λ 6328 Å). The incident beam could be polarized in any direction in a plane perpendicular to its direction of propagation. An analyzer placed between the holder and the plate provided any desired combination of polarized scatterings such as H_v and V_v polarizations.

None of our specimens gave a detectable H_v scattered intensity so that only V_v patterns and density fluctuations will be considered from here.

The intensity of scattered light was recorded in arbitrary units as a function of angle by means of the photometer which was designed and constructed for this purpose. The apparatus was similar to the one developed recently by Myers and Wims;¹⁵ the light source was a He-Ne laser (λ 6328 Å). The sample was held on the axis of a goniometer on the arm of which a photomultiplier was set. The instrument employs a photon counting detection method and is capable of both large and small angle measurements.

A two-pinhole collimator¹⁵ ahead of the photomultiplier allows the apparatus to work in full light.

Table I
Morphology Characterizing Parameters from Light Scattering and Electron Microscopy

% CTBN	Parameter					$2R, \mu$, averaged from E.M. ^a
	$2R, \mu$, from halo	a, μ	l_c, μ	v_c, μ^3	$2R, \mu$, from halo ^a	
5	No halo				No halo	0.94
9	4.16				No halo	1.10
14	4.32	2.25	1.93	50.27	4.35	
20	Monotonous scattering decrease	1.30	1.09	9.17	No halo	
28	4.4 ± 0.8	1.79	1.55	26.35	4.4	2.2 ± 0.8

^a W. D. Niegish, Union Carbide Corp., Bound Brook, N. J., kindly supplied these samples.

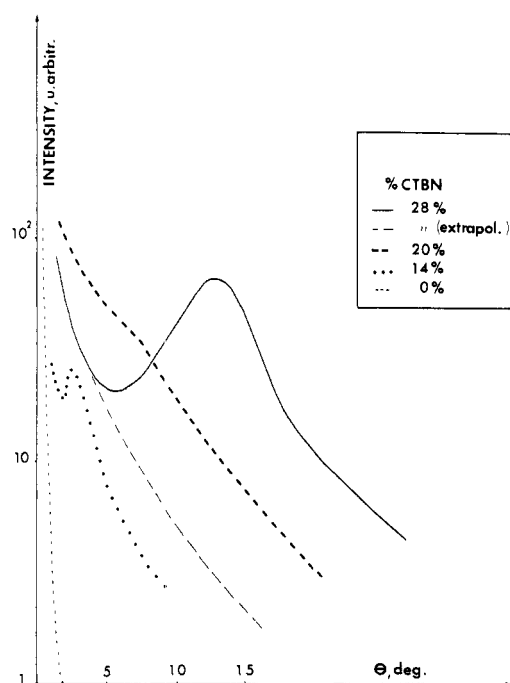


Figure 3. Scattered intensity vs. scattering angle θ . The extrapolated curve for the 28% sample was used to derive $\gamma(r)$.

Results and Discussion

Morphological Changes with CTBN Concentration.

Samples with increasing CTBN content were studied both photographically and photometrically. Some typical V_v patterns are shown in Figure 2 whereas the corresponding recordings along the scattering angle θ are shown in Figure 3. These results allow the determination of morphology characterizing parameters.

The appearance of a halo for $\theta = \theta_{\max}$ permits the evaluation of a diameter $2R$ of the particles (we will justify this procedure later on)

$$U = (4\pi R/\lambda) \sin \theta/2 = 5.76$$

with λ = wavelength within the medium, R = radius of scattering spheres, θ = scattering angle. The dispersion in size was checked by an analysis similar to the one used by Duplessix, *et al.*,¹⁰ assuming a Gaussian distribution, the experimental curve can be fitted with a theoretical one, except for small angles, where destructive interference produced a strong decrease in the observed intensity.

The classical Debye treatment⁶ (Fourier inversion of the smoothed intensity data with removal of maxima whenever

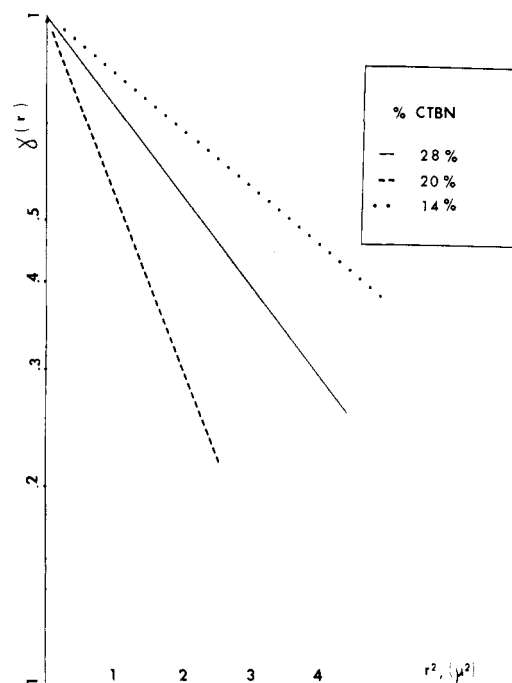


Figure 4. Plot of correlation function $\gamma(r)$ vs. r^2 .

a distinct peak was present) was used to calculate correlation functions $\gamma(r)$, which are shown in Figure 4. As $\gamma(r)$ could be relatively well fitted to a Gaussian function $\exp(-r^2/a^2)$ (cf. Figure 4), we took a as a qualitative estimate of the density fluctuation size in addition to the more usual parameters l_c and v_c .

Whereas the scattering pattern only shows a slight broadening of the transmitted beam for small CTBN concentrations, a weak halo appears in the 10% range. This is interpreted in terms of spherically shaped particles of micron range ($2R \sim 4 \mu$). At about 15% concentration, a second maximum sometimes appears at smaller angles probably meaning the smaller particles are packing into large domains.

For 20% CTBN, where phase inversion occurs, the density fluctuations are more frequent (a , l_c , and v_c show minimum values), and the scattering envelope shows only a continuous angular decrease of a high intensity scattering at small angles. After phase inversion, in the 25–30% CTBN range, spherical epoxy rich domains appear (cf. Figure 1b) and produce an intense circular maximum in the scattering pattern ($2R \sim 4.5 \mu$).

The qualitative agreement between the various param-

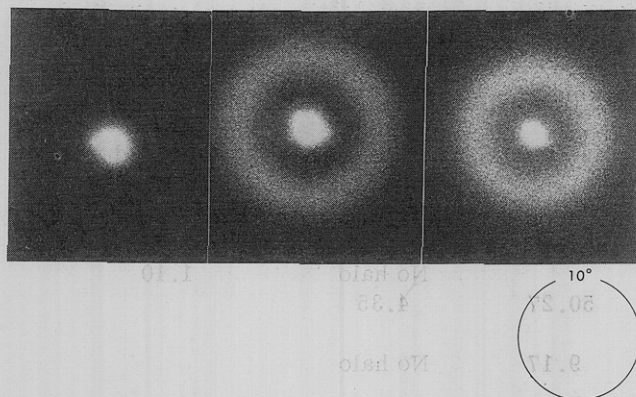


Figure 5. V_v scattering pattern after various curing times (28% CTBN): (left) 30 mn; (middle) 37 mn; (right) 45 mn.

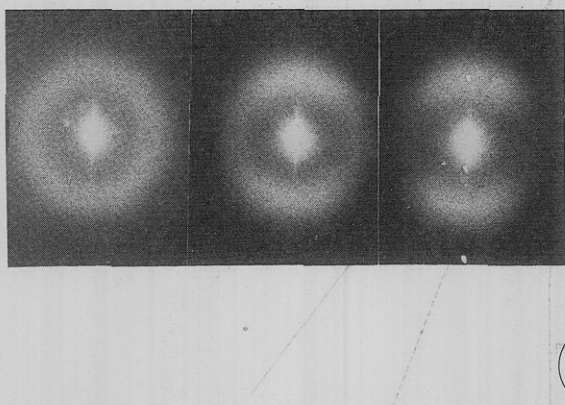


Figure 6. V_v scattering pattern after various static elongations (28% CTBN) (stretching axis horizontal): (left) 0%; (middle) 6%; (right) 18%.

ters in Table I is satisfactory. It is not surprising to get higher values for $2R$ from the LS than from the microscopy since: the thickness of the sections (1000–900 Å) is much smaller than the diameter of the particles, a single micrograph cannot give a quantitative value of the real size distribution. The large difference between the parameters calculated from the correlation function $\gamma(r)$ and the intensity maximum are not surprising either since $\gamma(r)$ includes short range fluctuations whereas the calculation of $2R$ assumes hard homogeneous spherical particles.

Morphological Changes During Polymerization. A special holder was built from a Kofler micro hot stage in order to study the light scattered when a sample is heated to a given temperature or is undergoing polymerization; a holder was designed to adapt the stage to the optical bench of the photographic apparatus and a glass cover was added to ensure proper temperature control inside the cell.

A first point to stress is the reproducibility of the observed morphology. In our case, a phase separation occurs for thermodynamic reasons at a certain stage of a chemical reaction whose kinetics can be easily controlled. This is to be compared with light scattering studies dealing with solvent cast films of block copolymers where the speed of evaporation of the solvent, a subtle parameter, controls the phase separation. The V_v scattering patterns after various polymerization times are shown in Figure 5 for a sample containing 28% CTBN. Table II summarizes the results obtained over a wide range of concentrations.

From these patterns, one can conclude that the polymerization starts with an induction period during which the mixture remains homogeneous. After about 30 min a phase

Table II
Changes of V_v Scattering Pattern During Polymerization

CTBN concn % in wt	Polymerization time, min	Diameter of halo, ^a mm
14	30	7
	35	7
	45	7
17	30	6.5
	35	6.5
	40	6.5
	45	6.5
20	30	No halo
28	30	6.5
	37	5.4
	45	4.5
33	30	8
	35	7.5
	40	6.5
	110	6

^a The film to sample distance was 140 mm. Curing temperature 120°.

separation occurs that can be followed on the scattering patterns except for the very low CTBN concentrations (where phase separation probably occurs in a range of sizes too small to be seen by LS). In most cases, the phase separation gives rise to a circular intensity maximum, the intensity of which increases rapidly.

As before, halos were observed corresponding respectively to spherical domains of epoxy or elastomer appearing in distinct ranges of CTBN concentration. These ranges are separated by a zone exhibiting an intense pattern in which the scattering decreases continuously with angle. It is interesting to stress that the kinetics of morphology development do not seem to vary with CTBN concentrations and that phase separation occurs well before the gelation point. The spherical shape of the particles and the low viscosity of the mixture, even after the phase separation, being evidence for this.

The further increase (after the gel point) of the scattered light by the whole sample is probably an artefact due to the appearance of small air bubbles in the cell at the glass–solid interface.

To explain the origin of the circular maximum in the scattering envelopes, one may evoke the following arguments. There are two distinct causes of a scattering maximum: (a) the shape of the particles, (b) the average distance between particles if a close packing effect gives rise to constructive interference between them. In passing from a dilute to a concentrated system where constructive interference occurs, the angular position ($U = 5.76$) of the secondary maximum (due to the spherical shape) does not change but that of the principal maximum moves from $U = 0$ to $U = 2.5$, depending on the concentration.¹⁶

In the present case, several arguments seem to favor the first hypothesis. The CTBN concentration has only a weak influence on the angular position of the maximum. (The micrographs show no evidence of clusters so that the particles are probably homogeneously dispersed; it is well known that closely packed spheres in a fixed volume contain a fixed quantity of matter so that such a morphology cannot cover a wide range of concentrations.) During the phase separation when the number of particles and the scattering intensity increase, the halo tends toward smaller angles or doesn't move, which cannot be explained in terms of constructive interference.

It is noteworthy that the phase inversion time, whatever this phase is, does not seem to be dependent on the CTBN content, at least in the range studied. This means that the thermodynamic conditions for the phase separation are essentially dependent on the degree of advancement of the chemical reaction of the epoxy and its hardener. The perfect independence of the gel point and the CTBN content accounting also for that.

Besides, phase separation is never complete; hundreds of small inclusions stay apart from the larger ones.

As there is no continuous change from these microscopic particles to the larger ones, we conclude that there are two types of particles occurring at different times. We suggest that even after the phase separation some elastomer stays dissolved in the continuous matrix and that this elastomer only separates later at a stage where the overall viscosity is much too large to allow association into spherical particles.

Morphological Changes During a Static Deformation. Simultaneous measurements of tensile stress and light scattering could be easily performed by placing the sample between the jaws of an Instron tester and having the sample illuminated by the laser beam. Figure 6 shows typical V_v patterns obtained for a sample containing 28% CTBN.

An H_v light scattering pattern could not be detected from any specimen at any degree of elongation.

The observed changes of the scattering patterns as a function of deformation are similar for all levels of CTBN. They show: a small deformation of the circular halo that changes into an ellipsoidal one, a sharp drop of intensity on the halo along the stretching direction. The Fourier transform of an ellipsoid with the major axis horizontal is an elliptical halo with its main axis vertical and of constant intensity. It would seem therefore that the particles change from spheres to ellipsoids on stretching. However this explains only partially the evolution of the scattering pattern, the variations of the intensity around the elliptical halo being an additional effect whose explanation probably rests in a correlated orientation of the particles in the direction of stretch. Thus one could propose rows of short rods made up of the ellipsoids, aligned in the direction of tension.

Conclusions and Perspectives

Heterogeneous spherical domains of ABE composites have been investigated by the light scattering technique under several experimental conditions. The results can be summarized as follows: (1) the variation in size and shape of the spherical particles (if any) with the CTBN content can easily be followed; besides, some additional parameters can characterize the heterogeneities at a much smaller level; (2) the phase separation has been studied in a continuous manner during the polymerization by means of a technique that could be applied to most gel-forming materials; (3) a preliminary investigation of the deformation mechanism is reported; the results are promising for relating the variation of intensity due to a sinusoidal stress to the value of $\tan \delta$.

Acknowledgments. The writers gratefully acknowledge the assistance of W. D. Niegish and A. C. Soldatos of the Union Carbide Research Laboratory of Bound Brook, N. J.

References and Notes

- (1) R. S. Stein and M. B. Rhodes, *J. Appl. Phys.*, **31**, 1873 (1960).
- (2) M. Moritani, N. Hayashi, A. Utsuo, and H. Kawai, *Polym. J.*, **2**, 74 (1971).
- (3) R. S. Stein, P. Erhardt, J. J. van Aartsen, S. Clough, and M. B. Rhodes, *J. Polym. Sci., Part C*, **13**, 1 (1966).
- (4) J. M. Charrier and R. H. Marchessault, *Fibre Sci. Technol.*, **5**, 263 (1972).
- (5) P. R. Sundararajan and R. H. Marchessault, *J. Mol. Biol.*, **63**, 305 (1972).
- (6) P. Debye and A. M. Bueche, *J. Appl. Phys.*, **20**, 518 (1949).
- (7) H. Keskkula and W. J. Frazer, *J. Polym. Sci., Part C*, **7**, 1 (1968).
- (8) M. Moritani, T. Inoue, M. Motegi, and H. Kawai, *Macromolecules*, **3**, 433 (1970).
- (9) T. Inoue, M. Moritani, T. Hashimoto, and H. Kawai, *Macromolecules*, **4**, 500 (1971).
- (10) R. Duplessix, C. Picot, and H. Benoit, *Polym. Lett.*, **9**, 321 (1971).
- (11) F. J. McGarry, AIAA/ASME 10th Structures, Structural Dynamics and Materials Conference, New Orleans, La., April 14–16, 1969.
- (12) A. C. Soldatos and A. S. Burhans, *Advan. Chem. Ser.*, **No. 99**, 531 (1971).
- (13) W. D. Niegish, Union Carbide Corp., Boundbrook, N. J., private communication.
- (14) J. Borch and R. H. Marchessault, *J. Polym. Sci., Part C*, **28**, 153 (1969).
- (15) M. E. Myers and A. M. Wims, *J. Colloid Interface Sci.*, **39**, 447 (1972).
- (16) A. Guinier and G. Fournet, "Small Angle Scattering of X-Rays," Wiley, New York, N. Y., 1955.

Surface Chemical Properties of Highly Fluorinated Ethylenic Polymers¹

Marianne K. Bernett

Laboratory for Chemical Physics, Naval Research Laboratory, Washington, D. C. 20375.
Received May 5, 1974

ABSTRACT: Wetting properties of seven new, well-characterized, highly fluorinated linear polymers were investigated. Fluorination in the polyethylene backbone was varied by degree of fluorine atom substitution; *n*-alkyl side chains of increasing number were fully fluorinated, whereas phenyl side groups were either fully fluorinated or non-fluorinated. Critical surface tensions of wetting obtained on thin cast films of these fluoropolymers were compared to those of polymers with related structures and surface constitutions. Because of the pressure of the bulky fluorine atoms and aromatic side groups, some of these molecules are extremely sterically blocked, which makes the prediction of an equilibrium surface conformation very difficult. The results are discussed in terms of solid surface constitution, steric hindrance, and electrostatic dipole contribution.

Highly fluorinated linear polymers are characterized by a low free surface energy and concomitant low wettability, as evidenced by the large contact angles of drops of organic and aqueous liquids. A comprehensive set of workable prin-

ciples had been built up by Zisman and coworkers relating the chemical and spatial constitution in the outermost surface of a polymer with its surface energy.² During the last few years Wall, Brown, and Lowry of the National Bureau